Linewidth broadening due to longitudinal spatial hole burning in a long distributed feedback laser

MingChiang Wu, Yuhwa Lo, and Shyh Wang

Citation: Applied Physics Letters **52**, 1119 (1988); doi: 10.1063/1.99180
View online: http://dx.doi.org/10.1063/1.99180
View Table of Contents: http://scitation.aip.org/content/aip/journal/apl/52/14?ver=pdfcov
Published by the AIP Publishing

Linewidth broadening due to longitudinal spatial hole burning in a long distributed feedback laser

Ming-Chiang Wu, Yu-hwa Lo, and Shyh Wang
Department of Electrical Engineering and Computer Science, Electronics Research Laboratory and Lawrence Berkeley Laboratory, University of California, Berkeley, California 94720

(Received 16 November 1987; accepted for publication 1 February 1988)

The spectral linewidth of a long distributed feedback (DFB) laser above threshold at high output power is investigated theoretically. Longitudinal spatial hole burning (LSHB) is shown to have important effects on the lasing characteristics and the broadening of linewidth. A four-wave coupled mode equation is developed to describe the LSHB phenomenon. The threshold gain and the carrier distribution are solved self-consistently above threshold at various output powers. The simulation results show that the power-linewidth product can increase by a factor greater than 2 due to LSHB for long DFB lasers. This theory has important implications on the limits of linewidth reduction by increasing the length of DFB lasers and on possible future device design for coherent optical system.

Recent interests in coherent optical communications have stimulated a great number of research papers on narrow linewidth semiconductor lasers.[1–5] Narrow linewidth laser source and local oscillator are the most important elements to achieve low bit error rate. Broad linewidth will degrade the receiving sensitivity. The degradation can be alleviated by using a higher modulation rate. The present realizable rate, however, is limited by the device response and parasitics and is of the order of 1 Gbit/s. In this case a linewidth smaller than 10 MHz is necessary for heterodyne frequency shift keying (FSK) and 1 MHz for heterodyne differential phase shift keying (DPSK) and phase shift keying (PSK).[1]

Several approaches for reducing the linewidth of semiconductor lasers have been reported, including external cavity with grating feedback,[2] extended fiber cavity,[3] integrated long passive cavity,[4] and long distributed feedback (DFB) lasers.[5] Although narrow linewidth has been achieved by the external cavity approaches, it depends critically on the phase of the externally reflected light. Furthermore, any residual reflections from the optical components will complicate the phase interference. On the other hand, the long DFB laser is particularly attractive because the mode and the linewidth are stable. A linewidth of 12 MHz has been reported for a 820-μm-long DFB laser.[5] In a theoretical analysis at the threshold condition, Kojima *et al.* showed that for a strongly coupled (large κL) DFB lasers without facet reflection the linewidth $\Delta\nu$ is proportional to $1/\kappa^2 L^3$, where κ is the coupling coefficient of the grating and L is the laser length.[6] Above threshold, however, the gratings confine most of the photons near the center of the laser, and the prediction based on the analysis at the threshold is no longer valid. Therefore, a theory is needed for linewidth of DFB lasers above threshold.

The purpose of this letter is to study possible fundamental limitations on the DFB laser linewidth. We show that for a DFB laser without facet reflectivity, the reduction of the linewidth with the laser length will be slower than $1/L^3$ due to longitudinal spatial hole burning (LSHB). In a long DFB laser, the carriers depleted by photons near the center induce a change of effective refractive index along the cavity. As a result, the effective reflectivity drops and the linewidth becomes broader. Such LSHB effect is analyzed self-consistently for a GaAs/AlGaAs DFB laser with spatially varying rate equations and four-wave coupled mode equations.

The structure of a DFB laser without facet reflectivity is shown schematically in Fig. 1(a). The periodic grating induces a perturbation on the propagation constant, $\Delta\beta = 2\kappa\cos(2K_B z)$, where K_B is the Bragg wave number. Figure 1(b) shows the distribution of photons and 1(c) shows the carrier distribution (solid line), which has a dip at

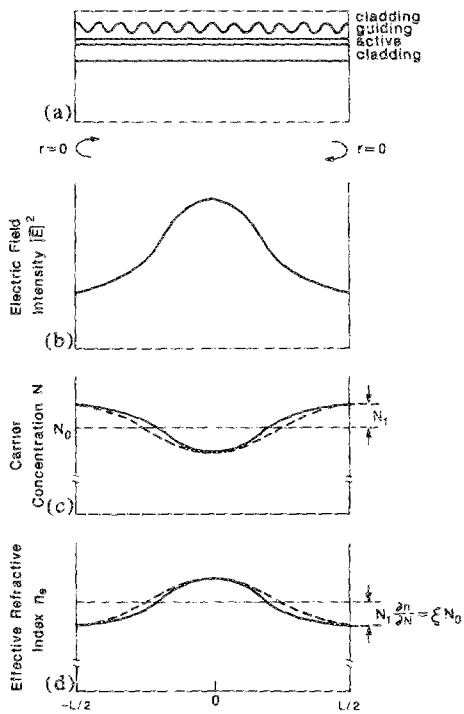

FIG. 1. (a) Schematic diagram of a DFB laser without facet reflectivity. (b) The electric field intensity distribution. (c) The carrier concentration distribution (solid line). (d) The distribution of the effective refractive index (solid line). The dotted lines in (c) and (d) are the sinusoidal approximations of the distribution.

 0003-6951/88/141119-03$01.00

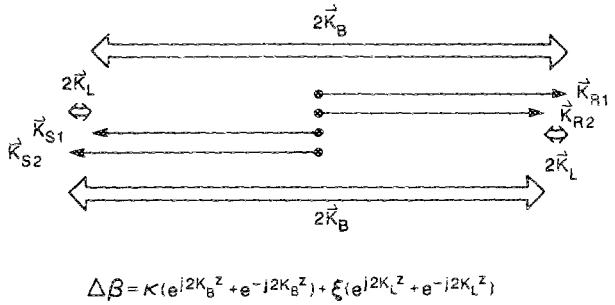

FIG. 2. Vector representation of Bragg reflection and LSHB scattering for a long DFB laser.

the center due to stimulated emission. The depleted carrier distribution can be approximated by a sinusoidal variation $\Delta N = N - N_0 = N_1 \cos(2K_L z)$, as is shown by the dotted line in Fig. 1(c), where N_0 is the average carrier concentration and $K_L = \pi/L$ is the LSHB wave number. The parameter N_1 depends on the photon density and hence on κ. The change in the effective refractive index n_e is proportional to the carrier concentration and is shown in Fig. 1(d). The propagation constant is modified by the additional factor $[1 + (2\xi/\beta_0)\cos(2K_L z)]$ due to the change of n_e, where $\xi = (N_1/n_e)(\partial n/\partial N)$ represents the strength of the LSHB-induced scattering, just as κ represents the strength of the Bragg reflection. Now $\Delta\beta(z) = \beta(z) - \beta_0 = 2\kappa\cos(2K_B z) + 2\xi\cos(2K_L z)$, neglecting the second order terms. The vector representations of both Bragg reflection and LSHB scattering are shown in Fig. 2. Since $K_L \ll K_B$, the LSHB scattering occurs only between waves propagating in the same direction and with wave numbers differing by $2K_L$. From the diagram we can see that the four waves are coupled together. The electric field can be written as

$$E(z) = R(z)e^{-jK_B z} + S(z)e^{jK_B z} \tag{1}$$

$$= [R_1(z) + R_2(z)e^{j2K_L z}]e^{-jK_B z} + [S_1(z) + S_2(z)e^{j2K_L z}]e^{jK_B z}, \tag{2}$$

where $R(z)$ and $S(z)$ represent the wave propagating in the $+z$ and $-z$ directions, respectively. The component $R(z)$ can be further decomposed into two waves coupled by LSHB, $R_1(z)$ and $R_2(z)$. Similarly $S(z)$ is decomposed into $S_1(z)$ and $S_2(z)$. Substituting $E(z)$ into the Maxwell's equation

$$\frac{d^2E}{dz^2} - \gamma_0^2 E = -j2\gamma_0\Delta\beta E, \tag{3}$$

we obtain the four-wave coupled mode equations

$$\frac{d}{dz}\begin{pmatrix} R_1 \\ S_1 \\ R_2 \\ S_2 \end{pmatrix} = \begin{pmatrix} g+j\delta & -j\kappa & -j\xi & 0 \\ j\kappa & -(g+j\delta) & 0 & j\xi \\ -j\xi & 0 & (g+j\delta)-j2K_L & -j\kappa \\ 0 & j\xi & j\kappa & -(g+j\delta)-j2K_L \end{pmatrix}\begin{pmatrix} R_1 \\ S_1 \\ R_2 \\ S_2 \end{pmatrix}, \tag{4}$$

where γ_0 is the complex propagation constant $g - j\beta_0$. If R_1, R_2, S_1, and S_2 vary as $e^{\pm pz}$ and since $\xi \ll \kappa$, the e^{+pz} component of the solution of the coupled mode equation $(R_1,S_1,R_2,S_2) \propto (l,s,t,su)e^{+pz}$, where $p^2 = (g+j\delta)^2 + \kappa^2$, $\delta = K_B - \beta$, and

$$s = \frac{j\kappa}{p + (g+j\delta)}, \quad t = -\frac{\xi}{2K_L}\frac{(g+j\delta)+j\kappa}{p+jK_L},$$

$$u = -\frac{\xi}{2K_L}\frac{(g+j\delta)-j\kappa}{p+jK_L}. \tag{5}$$

s is the effective reflectivity due to DFB grating while t and u are effective reflectivities due to LSHB. The e^{-pz} component is obtained from the symmetry condition $E(-z) = \pm E(z)$. Putting the $e^{\pm pz}$ components together, $R(z)$ and $S(z)$ can be written as

$$R(z) = (1 + te^{j2K_L z})e^{pz} \pm s(1 + ue^{-j2K_L z})e^{-pz}, \tag{6}$$

$$S(z) = s(1 + ue^{j2K_L z})e^{pz} \pm (1 + te^{-j2K_L z})e^{-pz}. \tag{7}$$

For antireflection-coated facet, the boundary condition $R(L/2) = R(-L/2) = 0$ gives the round trip condition

$$s^2\left(\frac{1-u}{1-t}\right)^2 e^{2pL} = 1. \tag{8}$$

Compared with the ideal DFB without LSHB the effective reflectivity s is modified by the factor $(1-u)/(1-t)$.

The threshold gain g_{th} is solved self-consistently from the round trip condition Eq. (8) with N_0 and N_1 calculated from the steady-state spatially varying rate equations. Figure 3 shows the magnitude of the modified effective reflectivity $s^2_{MOD} = s^2(1-u)^2/(1-t)^2$ with respect to the detuning from Bragg wave number δ at 0.1 mW ($g_{th} = 1.10\ \text{cm}^{-1}$) and 2.0 mW ($g_{th} = 1.48\ \text{cm}^{-1}$). At low output power (0.1 mW), the s^2_{MOD} is very similar to that without LSHB. With increasing power, there are strong perturbations on s^2_{MOD} at two sides of the stopband. The two lowest order modes, located near the valleys of the $|s_{MOD}{}^2|$ vs δ curve, are no longer degenerate. The effective reflectivity of the mode below the stopband is always higher than that

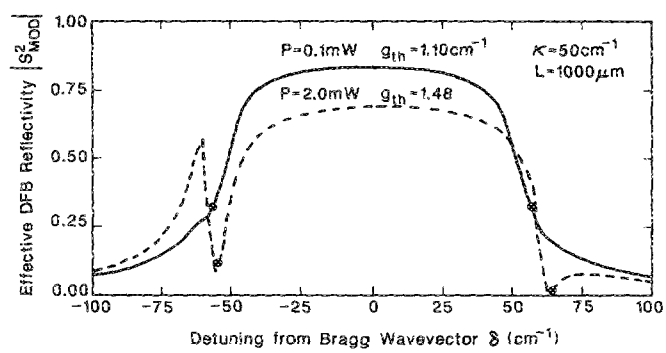

FIG. 3. Magnitude of the modified effective reflectivity $|s_{MOD}|^2$ vs the detuning from the Bragg wave number δ at 0.1 mW and 2 mW. The dots indicate the position of the lowest order modes.

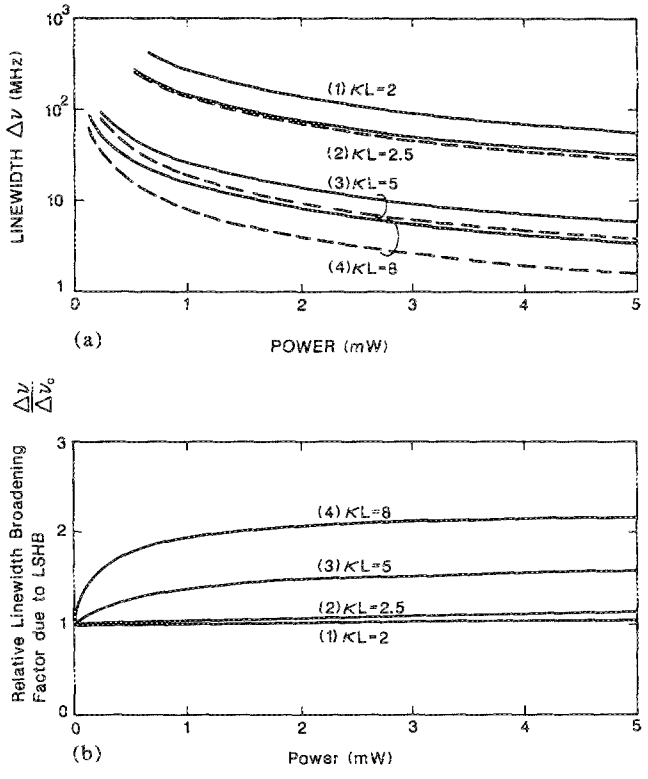

FIG. 4. (a) Spectral linewidth $\Delta\nu$ vs power P for four different coupling strength. The dotted lines show the linewidth without considering LSHB ($\Delta\nu_0$) and the solid lines show the effects of LSHB ($\Delta\nu$). (b) The relative linewidth broadening factor $\Delta\nu/\Delta\nu_0$ due to LSHB vs power P. The $[\kappa(\text{cm}^{-1}), L(\mu\text{m})]$ are [50,400], [50,500], [50,1000], and [80,1000] for curves (1), (2), (3), and (4), respectively.

above the stopband. Therefore, the laser tends to lase in the first mode below the stopband when LSHB occurs. This has been experimentally confirmed by Yamaguchi *et al.*[7] Furthermore, the effective reflectivity drops with increasing power since the strength of LSHB scattering $\xi = (N_1/n_e)(\partial n/\partial N)$ increases with power. As a result, the linewidth becomes broader as compared with that without considering LSHB.

The linewidth of the DFB laser is calculated from the g_{th} as in Ref. 8, assuming an internal loss of 50 cm^{-1}. The linewidth $\Delta\nu$ versus power P for LSHBed DFB laser is shown by the solid line in Fig. 4(a). The linewidth $\Delta\nu_0$ without considering LSHB is shown in the dotted line. The coupling strength κL varies from 2 to 8. For small κL ($\lesssim 2$), $\Delta\nu$ and $\Delta\nu_0$ are almost identical. When the coupling is stronger, the discrepancy between them becomes larger. Figure 4(b) shows the relative linewidth broadening factor $\Delta\nu/\Delta\nu_0$ vs power P. The ratio is almost unity for small κL at all powers. For larger κL, it increases rapidly with power and reaches a saturated number depending on the value of κL. The saturation with power is because the nonuniformity of the photon distribution is relaxed by the LSHB scattering. For $\kappa = 80$ cm^{-1} and $L = 1000$ μm, a factor greater than 2 is observed at 2 mW.

Without considering LSHB the linewidth reduction follows approximately the $1/L^3$ law. The LSHB changes the dependence to about $1/L^2$ at high powers. Therefore, in order to achieve the 1 MHz linewidth required for coherent optical communications, the devices must be designed to suppress the LSHB. High reflection coating on one facet of DFB laser has a more uniform field distribution. Passive reflecting gratings such as distributed Bragg reflector (DBR) laser structure is also favorable. On the other hand, the LSHB will be stronger for quarter-wave-shifted DFB lasers. The photon distribution is more nonuniform than conventional DFB lasers due to higher effective reflectivity.

In conclusion, we have shown that in a long DFB laser, the longitudinal spatial hole burning effect will increase the threshold gain and broaden the linewidth. Also the laser tends to lase in the first mode below the stopband. All these effects become more prominent for stronger coupling strength and higher output power. A relative linewidth broadening factor of 2 due to LSHB is predicted for $\kappa = 80$ cm^{-1} and $L = 1000$ μm at 2 mW output power. Device structures having more uniform field distribution and thus less LSHB are suggested.

This work was supported by National Science Foundation grant No. ECS-8410838, Eastman Kodak, Bell Communications Research and National Aeronautics and Space Administration grant No. NAG-1-580.

[1] J. Salz, AT&T Tech. J. **64**, 2153 (1985).
[2] R. Wyatt and W. J. Devlin, Electron. Lett. **19**, 110 (1983).
[3] T. P. Lee, S. G. Menocal, and H. Matsumura, Electron. Lett. **21**, 655 (1985).
[4] N. K. Dutta, T. Cella, J. L. Zilko, A. B. Piccirilli, R. L. Brown, and S. G. Napholtz, Appl. Phys. Lett. **50**, 644 (1987).
[5] K. Kojima, S. Noda, S. Tai, K. Kyuma, K. Hamanaki, and T. Nakayama, Appl. Phys. Lett. **49**, 366 (1986).
[6] K. Kojima, K. Kyuma, and T. Nakayama, IEEE J. Lightwave Technol. **LT-3**, 1048 (1986).
[7] M. Yamaguchi, T. Numai, Y. Koizumi, I. Mito, and K. Kobayashi, *Proceedings of 1987 Optical Fiber Communication Conference* (Optical Society of America, Washington, DC, 1987), p. 51.
[8] C. H. Henry, IEEE J. Quantum Electron. **QE-18**, 259 (1982).